Deep Learning-augmented SHS Model for Accurate AoI Analysis in Heterogeneous Unsaturated CSMA Networks

Suyang Wang, Yu Cheng
Department of Electrical and Computer Engineering, Illinois Institute of Technology, Chicago, 60616, USA
Email: swang133@hawk.iit.edu; cheng@iit.edu

IEEE INFOCOM 2025 - IEEE Conference on Computer Communications | 979-8-3315-4305-1/25/$31.00 ©2025 IEEE | DOI: 10.1109/INFOCOM55648.2025.11044711

***Abstract*—Accurate analysis of the age of information (AoI) is crucial for timeliness-critical systems that often rely on carrier sense multiple access (CSMA) networks. Existing models that minimize the tagged node's AoI in CSMA networks, where nodes contend for channel access, perform well with near-saturated background traffic but struggle in heterogeneous unsaturated networks. To address this, we propose a deep learning (DL)-augmented stochastic hybrid systems (SHS) model for fast and precise AoI analysis. Our approach aggregates background nodes into a single virtual saturated group while reflecting their heterogeneous and unsaturated characteristics via the channel access rate. By leveraging DL, the access point (AP) augments the SHS model with locally monitored traffic, enabling the tagged node to achieve precise AoI analysis. This integration significantly improves SHS precision, leading to accurate AoI estimation in heterogeneous and unsaturated settings. Validation through 802.11-based simulations in the ns-3 simulator demonstrates our model's robustness and efficiency in practical CSMA network scenarios. Additionally, we introduce a joint evaluation metric to balance AoI and sampling cost, ensuring an optimal trade-off between information freshness and resource consumption.**

***Index Terms*—Age of information, stochastic hybrid systems, carrier sense multiple access, deep learning, performance optimization.**

I. Introduction

Timeliness-critical systems underscore the importance of the age of information (AoI), a crucial metric for information freshness. It is defined as the elapsed time since the generation of the most recent update received by a destination node. The AoI captures the combined effects of source sampling rates and packet delivery latencies on information timeliness.

AoI has been analyzed using traditional graphical methods within various queuing and service frameworks. These methods have included studies on AoI in standard first-come-first-serve (FCFS) queuing systems, as well as more intricate environments [1]–[6]. Such investigations offer valuable insights into the impact of different queuing policies on AoI, particularly in contexts where queue delays and packet latencies are significant. Despite their usefulness, these traditional methods often encounter limitations when applied to more complex scenarios, such as those found in carrier sense multiple access (CSMA) networks, where nodes interact dynamically.

A stochastic hybrid system (SHS) approach is a powerful tool for analyzing average AoI, employing a continuous-time Markov chain (CTMC) framework. This method integrates CTMC state distributions with age resets occurring during discrete state transitions, alongside continuous dynamics representing AoI evolution within each state. This combination offers a robust and comprehensive understanding of AoI behavior in complex systems. By solving a system of balance equations, SHS facilitates more effective AoI analysis.

Given the critical role of CSMA networks in timeliness-sensitive applications, understanding and analyzing the AoI in these settings is essential. Kaul et al. [7] are among the first to investigate minimizing system age in CSMA-based vehicular networks by employing a small buffer and optimized broadcast periods without modifying existing hardware. However, their approach relies on simulation-based analysis, lacking theoretical underpinnings. Li et al. [8] advance the field by developing a Markov transmission model to evaluate AoI in CSMA networks, considering transmission and collision probabilities, packet rates, and node quantities, although limited to homogeneous settings. Conversely, Maatouk et al. [9] propose an SHS-based framework for AoI analysis in collision-free heterogeneous CSMA networks. This model assumes instant sampling and immediate preemptive service, neglecting practical queuing effects. They also approximate collision effects through bounded channel access time without evaluating performance in collision-prone environments. To bridge these gaps, Wang et al. [10] develop an SHS model (referred to as near saturated-SHS or NS-SHS in the following context) for heterogeneous CSMA networks that incorporates packet collisions and limited buffer scenarios. Nevertheless, this model's applicability is confined to near-saturated heterogeneous background nodes, meaning they almost always have packets ready for transmission, limiting its relevance in more realistic, unsaturated conditions.

To address these limitations, we propose a novel deep learning (DL)-augmented SHS model designed to enhance the precision of AoI analysis for a tagged node in heterogeneous unsaturated CSMA networks. Specifically, to construct a tractable finite-state system, we adopt the technique from [10] that aggregates all N background nodes into a single virtual saturated node, considering there always exists a certain background node contending for the channel when N is large enough. While this approximation significantly reduces the state dimension of the SHS system, accurately computing this virtual saturated background node's channel access rate R_b

is challenging, requiring dynamically knowing the number of nodes that actually contend the channel. One key contribution of this paper is to develop a data-driven machine learning (ML) approach to timely and accurately estimate R_b, which reflects the actual saturation degree of the background nodes. The other key component for accurate AoI analysis is the tagged node's collision probability p. It is impacted by both the traffic arrival rate of the tagged node and R_b, making it again significantly different from that in the saturated case.

To obtain R_b and p, we leverage DL to model the complex relationships between network dynamics and these variables. Specifically, inspired by [11], we use the AP's locally computed traffic received rates for each background node j, $\boldsymbol{\sigma} = \{\sigma_j\}_{j=1}^{N}$, and the tagged node's traffic arrival rate λ_t as inputs $\mathcal{X}^{(i)} = \{\boldsymbol{\sigma}, \lambda_t\}$ to the DL model, which predicts p and R_b as outputs $\boldsymbol{y}^{(i)}$. A key innovation we proposed for training data collection is the inverse calculation method, which is critical for generating accurate ground truth data for R_b by inversely solving SHS equations. By offloading DL inference to the AP, we reduce the computational burden on the tagged node while enabling efficient predictions. Finally, the tagged node's average AoI is computed by solving balance equations derived from the DL-augmented SHS.

To the best of our knowledge, we are the first to holistically integrate deep learning with SHS-based AoI analysis to enhance the precision of AoI predictions in heterogeneous unsaturated CSMA networks. This integration allows for rapid and precise adjustments of SHS parameters, ensuring the model adapts to varying network conditions while maintaining high accuracy in AoI predictions. Our ns-based simulations demonstrate the efficacy and accuracy of our DL-augmented SHS model, which outperforms existing approaches in heterogeneous unsaturated CSMA networks. Furthermore, we introduce a joint evaluation metric to balance AoI and sampling cost, enabling an optimal trade-off. Our contributions are multi-fold:

1) We examine the existing SHS-based approach for AoI analysis in CSMA networks, providing insights into its effectiveness in near-saturated scenarios and highlighting its limitations in unsaturated conditions.
2) We propose an innovative DL-augmented SHS model that enhances the accuracy of AoI analysis in heterogeneous unsaturated CSMA networks. Specifically, this model maintains tractability by aggregating background nodes into a single group and using virtual saturation assumptions. Leveraging deep learning, it captures complex network dynamics for fast, adaptable, and precise SHS parameter predictions, making it suitable for practical AoI estimation in real-world unsaturated CSMA networks. The ground truth for DL training is derived through direct measurements and a novel inverse calculation method based on SHS balance equations.
3) Our work is the first to holistically integrate CSMA MAC protocol analysis, machine learning, and SHS into a comprehensive AoI analytical system. This integration exemplifies the effective combination of domain knowledge with ML, a current trend in achieving powerful and practical solutions.
4) We validate the effectiveness and accuracy of our DL-augmented SHS model through extensive ns-3 simulations in 802.11-based networks. Our results show significant improvements in AoI analysis accuracy compared to existing approaches, particularly in heterogeneous unsaturated CSMA networks. Additionally, we balance AoI and sampling cost by defining a joint evaluation metric, ensuring an optimal trade-off between information freshness and resource consumption.

The paper is structured as follows: Section II introduces the system model, covering the general CSMA networking model and the fundamentals of AoI and SHS modeling for AoI analysis. In Section III, we present an insightful analysis of the existing NS-SHS model for AoI in CSMA. Section IV elaborates on the proposed DL-augmented SHS framework. Numerical results are detailed in Section V. Section VI reviews related work, and Section VII concludes the paper.

II. System Model

A. A General Unsaturated CSMA Network

In this study, we aim to develop an adaptive SHS-based model to dynamically evaluate the average AoI of the tagged node perceived by the monitor at the AP, incorporating accurate collision and traffic estimation over the CSMA MAC. The general CSMA network we consider involves one tagged node and N heterogeneous unsaturated background nodes sending informative updates to a monitor located at the AP via a shared wireless channel managed by the CSMA MAC protocol. The AP monitors the traffic received rates from all background nodes and uses this information to assist the tagged node in optimizing its arrival rate. To avoid hardware redesign or protocol modifications, each node sends packets through its local tail-drop FCFS MAC queue. The traffic arrival process at each queue follows a Poisson process, with different nodes having varying traffic arrival rates based on their demands. Before transmission, each node independently senses the channel. If the channel is idle, the node initiates an exponentially distributed backoff period and transmits a packet when the backoff ends. Successful transmissions or reaching the retransmission limit result in packet dequeues from the MAC queue, while collisions trigger retransmissions that go through the same backoff process. For mathematical tractability, we assume a constant channel capacity and exponentially distributed packet sizes. This CSMA setting is similar to that used in [10], which analyzes the AoI in a heterogeneous and near-saturated network. However, our work aims to develop a more practical model for scenarios regardless of the saturation degree of the background nodes. In our context, we refer to a node with a queue size of 1 as a "bufferless" node, indicating it can hold at most one packet at a time. Investigating a bufferless system is particularly valuable, as retaining old packets offers little benefit in terms of information freshness. Notably, the

model developed in this work is fully capable of accommodating a tagged node with a larger MAC queue, leveraging a similar modeling methodology as seen in [10]. However, for clarity and conciseness, we focus on the bufferless system to illustrate the core methodology.

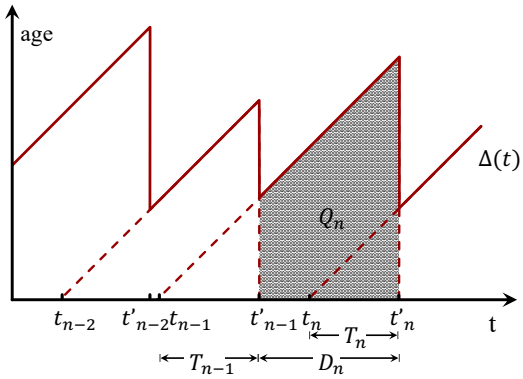

Fig. 1. Age waveform of a bufferless node.

B. SHS Basics for AoI Analysis

The age of information measures the time elapsed since the most recent update was generated. When a source creates update i with timestamp $u_i(t)$, it is sent through the system and eventually arrives at the monitor. The monitor observes its most recent update received at time t with an age of $t - u_i(t)$. As time progresses without new updates, the age increases linearly. The average AoI is the time-average of the instantaneous age waveform $\Delta(t)$, as depicted in Fig. 1. For a bufferless node, a new update arrival enters the system as long as the node is empty, and waits to be transmitted; otherwise, the new update will be dropped upon arrival. Thus, the time instant of the n^{th} arrival t_n is always no earlier than the $n-1^{th}$ departure instant t'_{n-1}. Over a sufficiently large time duration τ, the average AoI is given by $\langle\Delta\rangle_\tau = \frac{1}{\tau}\int_0^\tau \Delta(t)dt$. For the n^{th} delivered update, its inter-departure time and system time are denoted as $D_n = t'_n - t'_{n-1}$ and $T_n = t'_n - t_n$, respectively. The sum of each shaded area $Q_n = \frac{1}{2}D_n^2 + D_nT_{n-1}$ is equal to the integral denoted by $\langle\Delta\rangle$. The average AoI is

$$\Delta = \lim_{\tau\to\infty}\langle\Delta\rangle_\tau = \frac{E[Q_n]}{E[D_n]}. \tag{1}$$

For analytical details on applying equation (1) to different queuing systems, please refer to the tutorial article [12].

Although traditional graphical methods are commonly used, the SHS model offers an alternative approach to computing the average age in complex systems. This approach considers the networking system as a CTMC, facilitated by the assumption of exponential backoff and transmission duration. By establishing a set of balance equations that incorporate the CTMC state distributions, the age-increasing process in each state, and the age reset upon state transitions, we can solve for the average AoI [2], [13].

A Markov process $\vec{q}(t)$ can be represented as a Markov chain $(\mathbb{Q}, L)$, where $\mathbb{Q}$ denotes the set of states, and L represents the transition edges. Each transition has a rate denoted by $\lambda^{(l)}\delta_{\vec{q}_l,\vec{q}(t)}$, with outgoing and incoming transitions for each state defined as $L_{\vec{q}}$ and $L'_{\vec{q}}$ respectively.

In the SHS model, network events are managed by the Markov chain, while AoI evolution is handled by the continuous state process $\mathbf{x}(t)$. Transitions in the discrete state result in a reset in the continuous state, modeled by the transition reset matrix $\mathbf{A}_l$. The age process $\mathbf{x}(t)$ evolves linearly in each state $\vec{q} \in \mathbb{Q}$ and is governed by the differential equation $\dot{\mathbf{x}} = \mathbf{b}_{\vec{q}}$, where $\mathbf{b}_{\vec{q}}$ indicates whether the age increases or remains constant in each state.

To determine the average age using SHS, we define $\pi_{\vec{q}}(t)$ as the stationary probability distribution of the Markov chain and $\mathbf{v}_{\vec{q}}(t)$ as the correlation between the age process and the discrete state. Assuming the ergodicity of $\vec{q}(t)$, the steady-state probabilities $\bar{\pi}$ are found by solving the balance equations

$$\bar{\pi}_{\vec{q}}\left(\textstyle\sum_{l\in L_{\vec{q}}}\lambda^{(l)}\right) = \textstyle\sum_{l\in L'_{\vec{q}}}\lambda^{(l)}\bar{\pi}_{\vec{q}_l}, \quad \vec{q}\in\mathbb{Q}, \tag{2}$$

$$\textstyle\sum_{\vec{q}\in\mathbb{Q}}\bar{\pi}_{\vec{q}} = 1. \tag{3}$$

The convergence of $\mathbf{v}_{\vec{q}}(t)$ is then given by

$$\bar{\mathbf{v}}_{\vec{q}}\textstyle\sum_{l\in L_{\vec{q}}}\lambda^{(l)} = \mathbf{b}_{\vec{q}}\bar{\pi}_{\vec{q}} + \sum_{l\in L'_{\vec{q}}}\lambda^{(l)}\bar{\mathbf{v}}_{\vec{q}_l}\mathbf{A}_l, \quad \vec{q}\in\mathbb{Q}. \tag{4}$$

Finally, the average age Δ of the tagged node is calculated as

$$\Delta = \textstyle\sum_{\vec{q}\in\mathbb{Q}}\bar{v}_{\vec{q}0}. \tag{5}$$

III. Analysis of the NS-SHS Model

NS-SHS involves labeling the tagged node and representing a vector of the age processes as the continuous state to track the age of each update accordingly. We hereby briefly introduce the fundamentals of the SHS model from [10].

The states of the network is typically modeled by $(\vec{q}(t), \mathbf{x}(t))$, where

1) The discrete process $\vec{q}(t) \in \mathbb{Q}$ represents the state of the network at time t, with $\mathbb{Q}$ denoting the discrete set of possible states. Note that we use $\vec{q}(t)$ to denote the state, which takes the form of a pair of scalar values.
2) The vector $\mathbf{x}(t) = [x_0(t), x_1(t), \cdots x_K(t)]$ traces the age evolution of the tagged node's packets at the monitor and in the queue. Specifically, $x_0(t)$ is the age of the tagged node's latest update at the monitor. The tagged node's queue capacity is denoted as K, with packets in the queue indexed from 1 to K, where packet 1 is at the head of the queue.

A. NS-SHS for CSMA with Bufferless Nodes

The SHS fundamentals above are then applied for analyzing the AoI of a tagged node in a CSMA network containing one tagged node and N background nodes. Node i generates packets at a rate of λ_i following a Poisson process. These packets are then added to the transmission queue. Node i undergoes an exponentially distributed backoff procedure with an average duration of $1/R_i$. Once the backoff period ends, the packet begins transmission. The transmission time is also exponentially distributed, with an average duration of $1/H_i$.

A bufferless tagged node uses a transmission queue with a capacity of one packet, with an arrival rate λ_t. Thus, the tagged node's queue capacity K is set to 1. The N background nodes transmit with varying arrival rates. To create a tractable finite-state SHS, the model aggregates the impact of the N background nodes into a single state. Specifically, the network's state is denoted by a 2-tuple, where the first indicates the state of the tagged node, and the second element indicates the state of the background nodes. The set of possible states $\mathbb{Q} = \{(k, Q), (C, Q), (k, C)\}, k \in [0, 1]$. The states are specified as follows:

- $(1, Q)$: Both the tagged node and the background nodes are in the exponential backoff process, contending for channel access, with the tagged node having one packet waiting to be transmitted. "Q" indicates that the aggregated background node always has packets waiting to be transmitted and is always contending for the channel. After a successful transmission or a transmission failure due to reaching the retransmission limit by the background node, the state returns to "Q".
- $(0, Q)$: The tagged node has no pending packets, and only the background nodes are contending for the channel.
- (C, Q): The tagged node has completed the backoff procedure and is currently transmitting.
- (k, C): A background node has finished its backoff procedure before the tagged node and is occupying the channel for transmission.

State (C, C) is considered impossible to simplify the model without compromising its accuracy, as the actual collision impacts are adequately captured by the transitions caused by collisions during transmission.

State transitions occur under the following conditions:

- A new update enters the tagged node's queue, with an arrival rate of λ_t.
- One of the nodes captures the channel.
- A retransmission occurs due to a collision.
- A transmission is successful.

This model incorporates the collision effect by integrating the conditional collision probability p seen by the tagged node and the successful transmission probability $1 - p$ into the transition rates caused by collisions and successful transmissions, respectively.

The tagged node's age vector is $\mathbf{x} = [x_0, x_1]$, where x_0 represents the age of the latest received packet at the monitor, and x_1 represents the age of the packet in the tagged node's queue. Using the equations in Section II-B, we can calculate the average age. Please refer to [10] for calculation details.

B. Limitations for Unsaturated Scenarios

In this section, we discuss the limitations of the NS-SHS model regarding its effectiveness and adaptability to unsaturated CSMA networks.

As demonstrated in Section III-A, the NS-SHS model effectively incorporates the collision effect and aggregates the background nodes into a single state within the CTMC, achieving simplicity and tractability. The approximation of near-saturated background nodes allows the tagged node to determine its conditional collision probability p using classic analysis from [14], [15]. The channel access rate of the tagged node, R_t, can be formulated as $R_t = 1/(t_{slot} \cdot \bar{W})$, where $\bar{W}$ is the average contention window in terms of time slots and t_{slot} denotes the slot time. This formulation indicates the average channel access attempts per unit of time. Additionally, the aggregated background node's channel access time is the minimum of N exponential variables, resulting in the channel access rate of the aggregated background node being set to N times that of the tagged node, $R_b = NR_t$.

However, we argue that this approximation has significant limitations. Firstly, assuming the aggregated background node always has a packet to send, regardless of which background node is actually sending, differs from reality. In practice, the impact on the tagged node varies depending on whether all N background nodes or just a few of them are contending for the channel. Additionally, the channel access rate R_t obtained via saturated analysis cannot accurately reflect the tagged node's actual channel access rate. The NS-SHS model is more suitable for networks closer to the former scenario, where most background nodes are saturated. In contrast, as a network leans towards the latter scenario, where fewer background nodes contend for the channel, the NS-SHS model becomes increasingly inaccurate.

The limitations manifest in two key aspects:

- The NS-SHS model assumes a saturated network, leading to inaccuracies in calculating the collision probability p and, subsequently, the channel access rate R_t.
- The assumption $R_b = NR_t$ in NS-SHS is based on a saturated homogeneous approximation, which does not hold in unsaturated networks. In unsaturated networks, R_b can vary within the range $(0, NR_{\max}]$, where $R_{\max}$ is the maximum possible channel access rate considering no collisions. Here, $R_{\max} = 1/(t_{slot} \cdot C\bar{W}_{\min})$, where $C\bar{W}_{\min}$ denotes the average of initial contention window size.

IV. DL-augmented SHS

In heterogeneous and unsaturated contention-based CSMA networks, the interactions among nodes are complex and uncertain, making the quantitative evaluation of p and R_b particularly challenging. To address this, we propose a DL-augmented SHS framework that integrates real-time DL predictions into SHS analysis to enable precise AoI estimation and optimization.

A. Framework Overview

The DL-augmented SHS framework consists of three stages: DL Model Training, inference and SHS augmentation, and AoI calculation. Fig. 2a illustrates the overall process of the framework, excluding the detailed DL model training process. The framework centralizes inference and decision-making at the AP. The AP monitors traffic conditions, including the received rates from background nodes $\boldsymbol{\sigma} = \{\sigma_j\}_{j=1}^{N}$, and locally proposes the tagged node's arrival rate λ_t. These

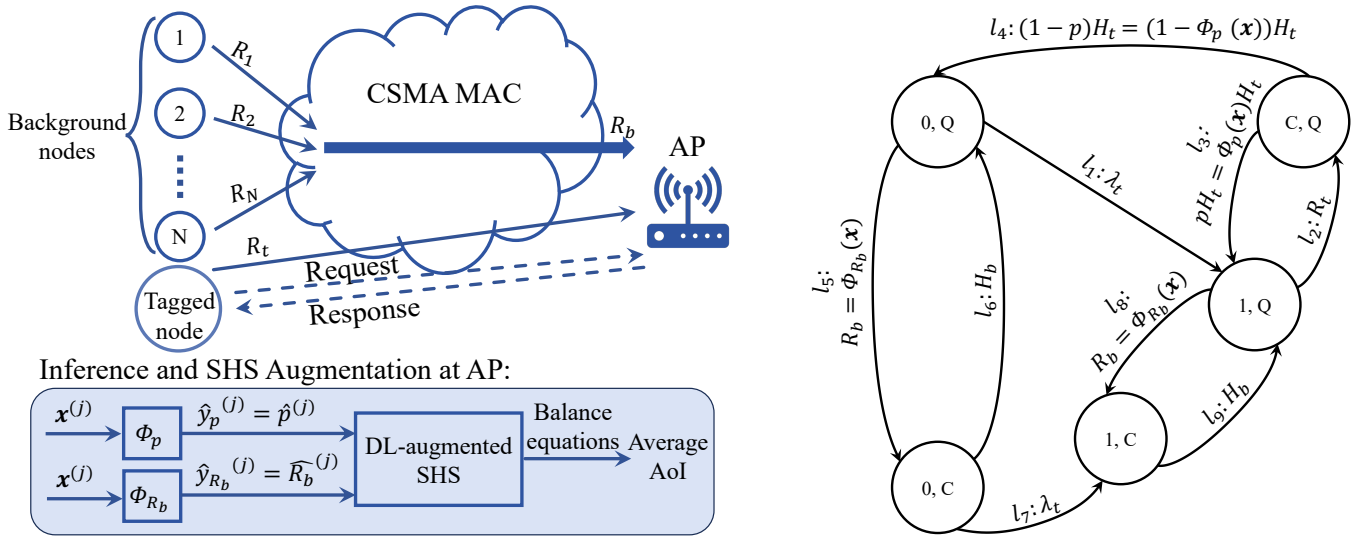

(a) DL-augmented SHS framework: The tagged node requests the optimal arrival rate λ_t from the AP, which hostsϕ_p and ϕ_{R_b} to predict p and R_b.

(b) The DL-augmented SHS CTMC.

Fig. 2. The DL-augmented SHS framework and the DL-augmented SHS CTMC.

parameters form the input vector $\mathcal{X} = \{\boldsymbol{\sigma}, \lambda_t\}$, which is fed into the DL models, ϕ_p and ϕ_{R_b}. These models predict the packet collision probability p and the background nodes' channel access rate R_b, which are used to augment the SHS model. The AP iteratively adjusts λ_t to optimize AoI and provides the tagged node with the optimal arrival rate.

By leveraging DL, the proposed framework refines SHS parameters, improving adaptability and precision in dynamic, unsaturated environments. Rather than directly predicting AoI, DL focuses on p and R_b, which are bounded (p by 1 and R_b by $NR_{\max}$), providing a more stable basis for DL outputs. Additionally, the SHS model, augmented with accurate parameters, supports analyses beyond AoI, making it versatile for broader performance evaluations.

B. DL Model Training

We propose training two separate deep learning models, ϕ_p and ϕ_{R_b}, offline to provide fast and precise predictions of the current channel conditions, specifically the collision probability p and the channel access rate R_b during runtime.

a) Input Features: The factors influencing p and R_b should be considered as candidates for the ML model input. Inspired by [11], [16], we select the traffic received rate at the AP from each background node because it encapsulates information about the arrival rate at each node's MAC queue, overall channel utilization, and the interactions among all CSMA nodes. This method simplifies the communication complexity, and requires only the deployment of an AP to monitor incoming traffic and respond to inquiries from the tagged node. The input features for the DL model include the traffic received rate at the AP from each background node, denoted by $\boldsymbol{\sigma} = \{\sigma_j\}_{j=1}^{N}$, and the packet arrival rate of the tagged node, λ_t. Thus, the input vector is $\mathcal{X} = (\sigma_1, \sigma_2, \ldots, \sigma_N, \lambda_t)$. The outputs of the DL model are p and R_b.

b) Training Datasets: We use two separate training datasets for the two DL models. The dataset $D_p \triangleq \{(\mathcal{X}^{(i)}, y_p^{(i)})\}_i$ is used to train the DL ϕ_p for inferring the collision probability p. Similarly, the dataset $D_{R_b} \triangleq \{(\mathcal{X}^{(i)}, y_{R_b}^{(i)})\}_i$ is used to train the DL ϕ_{R_b} for inferring the channel access rate R_b. Each dataset captures the historical results of past problem instances. Here, $\mathcal{X}^{(i)}$ represents the i^{th} input vector, and $y_p^{(i)}$ and $y_{R_b}^{(i)}$ are the ground truth values for the respective output parameters.

c) Obtaining Ground Truths: Ground truths for p and R_b are obtained through a combination of simulation and analytical methods:

For p: The ground truth for p is obtained directly through measurement in the simulation environment. By monitoring the packet transmission attempts and acknowledgments (ACKs), we can accurately determine the collision probability.

For R_b: The ground truth for R_b is obtained via the proposed inverse calculation method using the SHS balance equations. Given p, we can derive R_t as a function of p:

$$R_t = \frac{1}{t_{\text{slot}} \cdot \bar{W}}, \tag{6}$$

where the average contention window $\bar{W}$ is given by

$$\bar{W} = \sum_{k=1}^{a+1} p^{k-1}(1-p)^{I\{k<a+1\}} \sum_{j=1}^{k} \frac{CW(j)-1}{2}, \tag{7}$$

$$CW(k) = \min\left(2^m CW_{\min}, 2^{k-1} CW_{\min}\right), \quad k = 1, \ldots, a+1,$$

and $I\{A\}$ is an indicator function that is 1 if A is true, and 0 otherwise [17]. Given the average AoI of the tagged node is $\Delta = f(p, \lambda_t, R_t, R_b, H_t, H_b)$, since Δ and the other parameters are known at the moment, R_b can be inversely calculated as

$$R_b = f^{-1}(\Delta, p, \lambda_t, R_t, H_t, H_b),$$

TABLE I
SHS TRANSITIONS OF THE TAGGED NODE

l	l_1	l_2	l_3	l_4	l_5	l_6	l_7	l_8	l_9
$\vec{q}_l \to \vec{q}'_l$	$(0,Q) \to (1,Q)$	$(1,Q) \to (C,Q)$	$(C,Q) \to (1,Q)$	$(C,Q) \to (0,Q)$	$(0,Q) \to (0,C)$	$(0,C) \to (0,Q)$	$(0,C) \to (1,C)$	$(1,Q) \to (1,C)$	$(1,C) \to (1,Q)$
$\lambda^{(l)}$	λ_t	R_t	pH_t	$(1-p)H_t$	R_b	H_b	λ_t	R_b	H_b
$\mathbf{x}\mathbf{A}_l$	$[x_0, 0]$	$[x_0, x_1]$	$[x_0, x_1]$	$[x_1, 0]$	$[x_0, 0]$	$[x_0, 0]$	$[x_0, 0]$	$[x_0, x_1]$	$[x_0, x_1]$
$\mathbf{v}_{\vec{q}_l}\mathbf{A}_l$	$[v_{(0,Q)0}, 0]$	$[v_{(1,Q)0}, v_{(1,Q)1}]$	$[v_{(C,Q)0}, v_{(C,Q)1}]$	$[v_{(C,Q)1}, 0]$	$[v_{(0,Q)0}, 0]$	$[v_{(0,C)0}, 0]$	$[v_{(0,C)0}, 0]$	$[v_{(1,Q)0}, v_{(1,Q)1}]$	$[v_{(1,C)0}, v_{(1,C)1}]$

subject to

$$0 < R_b \leq NR_{\max}. \tag{8}$$

d) MLP Model Training: We train two separate multi-layer perceptrons (MLPs), ϕ_p and ϕ_{R_b}, to infer the collision probability p and the channel access rate R_b, respectively. The models are trained on their respective datasets, $D_p \triangleq \{(\mathcal{X}^{(i)}, y_p^{(i)})\}_i$ for ϕ_p and $D_{R_b} \triangleq \{(\mathcal{X}^{(i)}, y_{R_b}^{(i)})\}_i$ for ϕ_{R_b}, using mean absolute error (MAE) as the loss function:

$$\mathcal{L}(\hat{y}^{(i)}, y^{(i)}) = \frac{1}{n}\sum_{i=1}^{n}\left|\hat{y}^{(i)} - y^{(i)}\right|. \tag{9}$$

The training process minimizes

$$\mathcal{L}(\hat{y}^{(i)}(\boldsymbol{\theta}), y^{(i)}), \tag{10}$$

where $\hat{y}^{(i)} = \phi(\mathcal{X}^{(i)}; \boldsymbol{\theta})$ is the output produced by the DL model ϕ parameterized by $\boldsymbol{\theta}$. The models are validated on separate datasets to ensure accuracy.

C. Inference and SHS Augmentation

During runtime, the AP monitors $\boldsymbol{\sigma}$ and locally proposes λ_t. The AP assembles the input vector $\mathcal{X} = \{\boldsymbol{\sigma}, \lambda_t\}$ and feeds it into the trained DL models, ϕ_p and ϕ_{R_b}. These models predict p and R_b, which are used to augment the SHS model. By using these predictions, the SHS model is dynamically updated to reflect real-time network conditions, enabling accurate AoI estimation and informed decision-making.

D. AoI Calculation Using DL-augmented SHS

Fig. 2b illustrates the SHS CTMC for the bufferless tagged node under a CSMA network. The SHS transitions of the model are shown in Table I, with explanations below:

- l_1: A new update arrives at the empty MAC queue at rate λ_t. The state transitions from $(0,Q)$ to $(1,Q)$ without reducing age, so $x'_0 = x_0$ and $x'_1 = 0$. Thus, $\mathbf{x}\mathbf{A}_l = [x_0, 0]$ and $\mathbf{v}_{\vec{q}_l}\mathbf{A}_l$ is $[v_{(0,Q)0}, 0]$.
- l_2: The tagged node with a pending packet captures the channel at rate R_t. Since no update is delivered, $x'_0 = x_0$ and $x'_1 = x_1$.
- l_3: Transmission fails due to a collision at rate pH_t, leading to state transition back to $(1,Q)$. The collision probability p is predicted by the MLP ϕ_p.
- l_4: The update is successfully transmitted and received by the monitor at rate $(1-p)H_t$, reducing the age at the monitor to $x'_0 = x_1$.
- l_5: A background node captures the channel at rate R_b. This transition does not change x_1. R_b is predicted by the MLP ϕ_{R_b}.
- l_6: Background node transmission, whether successful or collided, completes at rate H_b, releasing the channel for new contention.
- l_7: A new update arrives at the tagged node's queue at rate λ_t during background node transmission, with no reset to $\mathbf{x}$.
- l_8: A background node captures the channel, with no change to the tagged node's age, $x'_1 = x_1$.
- l_9: A background node's transmission completes at rate H_b, again without affecting $\mathbf{x}$.

The age-increasing process in each state is indicated by $\dot{\mathbf{x}} = \mathbf{b}_{\vec{q}} = \begin{cases}[1 \quad 0], & \vec{q} = (0,*),\\ [1 \quad 1], & \text{otherwise.}\end{cases}$ This means the age x_0 always increases at a unit rate, while x_1 increases at a unit rate only in states other than $(0,*)$. The average AoI is then determined by solving the balance equations of the DL-augmented SHS model according to Section II-B. This enhanced SHS model ensures the estimated AoI closely approximates the true value under current network conditions.

Our framework adapts dynamically to real-time conditions, ensuring precise parameter estimation with minimal computational overhead and fast, accurate AoI estimation for diverse network scenarios.

V. NUMERICAL RESULTS

We evaluate our DL-augmented SHS model using ns-3 simulations [18]. This section outlines the simulation setup, MLP training process, and application of the trained MLP for refining the SHS model. We compare theoretical AoI estimations with simulation results for the IEEE 802.11 DCF protocol, demonstrating improved accuracy over the NS-SHS model in both unsaturated and saturated CSMA networks. We also explore the trade-off between sampling cost and AoI, introducing a joint evaluation metric to balance these factors.

TABLE II
NETWORK PARAMETERS

Parameter	Value
Slot time	$20\,\mu s$
DIFS	$50\,\mu s$
SIFS	$10\,\mu s$
Initial contention window size $CW_{\min}$	31
Maximum backoff stages	5
Maximum retransmission limit	7
Number of nodes	[1, 16]
Packet payload size	8,000 bits
Bit rate for DATA frame	11 Mbps
Bit rate for ACK frame	1 Mbps
Bit rate for PLCP & Preamble	1 Mbps
PHY header	192 bits
MAC header	224 bits
IP header	160 bits
ACK	112 bits + PHY header

A. Simulation Setup

For illustration purposes, we construct a CSMA network following the IEEE 802.11 distributed coordination function

TABLE III
MLP PARAMETERS

Parameter	Value ϕ_p	Value ϕ_{R_b}
# Input	16	16
# Output	1	1
Batch size	10	16
# hidden layers	4	3
# unit in layer 1	512	509
# unit in layer 2	512	371
# unit in layer 3	256	358
# unit in layer 4	256	N/A
# Epochs	1,000	1,000
Data size	38,000	38,000
Train, validation size	26,600, 11,400	26,600, 11,400
Optimizer	SGD	SGD
Activation function	ReLU	ReLU
Learning rate	5e-04	1.014e-05
Momentum	0.5	0.479
Early stopping patience	50	50

MAC protocol, with detailed configurations shown in Table II. Note that our proposed approach is general to all CSMA networks. To better focus on the core of our method, we do not consider hidden terminal problems.

Each node transmits one data frame for each transmission attempt. Each experimental run lasts 300 seconds, and the samples in the initial 50% of the simulation period are discarded to eliminate transient effects and ensure steady-state analysis. Our setting adopts a heterogeneous approach, with the traffic arrival rate of each background node randomly set from a uniform distribution with a maximum rate that varies for different numbers of background nodes to achieve various saturation degrees. With the simulation environment established, we proceed to train our MLP models to predict network parameters accurately.

B. MLP Training

To train a robust and general model capable of predicting target variables under varying network conditions, we conduct extensive simulations with different numbers of nodes and traffic rate patterns. We construct a training dataset with a maximum number of background nodes, denoted as $N_{\max}$, to ensure the ML models can handle a wide range of network scenarios. The input vector size is $N_{\max}+1$ and takes the form $\mathcal{X} = (\sigma_1, \sigma_2, \ldots, \sigma_{N_{\max}}, \lambda_t)$. Since the number of background nodes varies from instance to instance, we zero-pad the input values for scenarios with fewer than $N_{\max}$ background nodes. This maintains a consistent input vector size, ensuring that the MLP can handle any network scenario within the defined parameters.

Our training set consists of 38,000 instances generated via ns-3 simulations with $N_{\max} = 15$. A framework named Optuna [19] is used to optimize the hyperparameters, which are listed in Table III. The model is trained using PyTorch [20] with an early stopping scheme to prevent overfitting. In Fig. 3, we show the training process of ϕ_p and ϕ_{R_b}, demonstrating the good generalization and accurate prediction capability of the two MLPs across instances with various numbers of background nodes and traffic patterns.

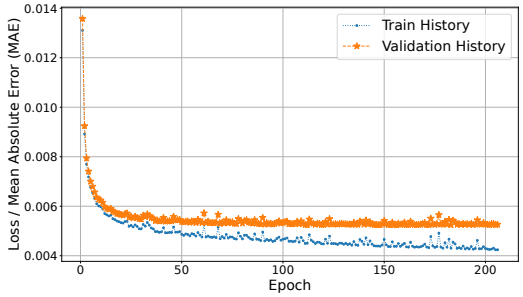

(a) MLP model ϕ_p.

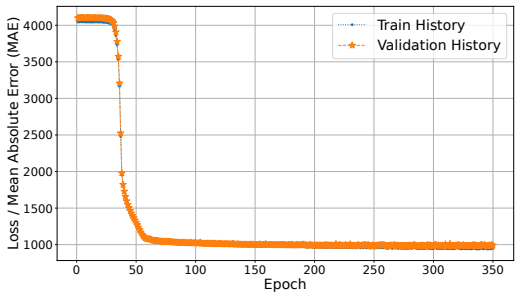

(b) MLP model ϕ_{R_b}.

Fig. 3. MLP training: MAE vs. epochs.

C. Accuracy Validation and Performance Comparison

We evaluate the performance of our proposed DL-augmented SHS model in terms of its accuracy in AoI prediction under both unsaturated and saturated scenarios. Additionally, we demonstrate the superiority of our model over NS-SHS in unsaturated networks.

a) AoI in Unsaturated Networks: Fig. 4 shows the average AoI versus the tagged node's arrival rate in unsaturated CSMA networks with 5, 10, and 15 background nodes, respectively. For illustration purposes, these figures represent AoI sampled with background nodes' traffic arrival rates chosen from a predefined narrow range, ensuring a consistent and stable saturation degree. As expected, the AoI decreases as the arrival rate λ_t increases. Higher arrival rates lead to more frequent updates, thereby keeping the information fresher. The bufferless setting reduces queueing delay, resulting in a monotone decreasing trend. The AoI curves obtained by our proposed DL-augmented SHS method closely match the simulation results across all samples, demonstrating its great accuracy and robustness in unsaturated cases. In contrast, the gap between the simulation and the NS-SHS results highlights the limitations of NS-SHS in analyzing unsaturated CSMA networks.

b) AoI in Saturated Networks: Fig. 5 demonstrates the applicability of the DL-augmented SHS to saturated CSMA networks. The AoI results obtained by our proposed SHS method, the simulation, and the NS-SHS are very close across all samples, indicating the effectiveness of our model in heterogeneous saturated scenarios with various network settings.

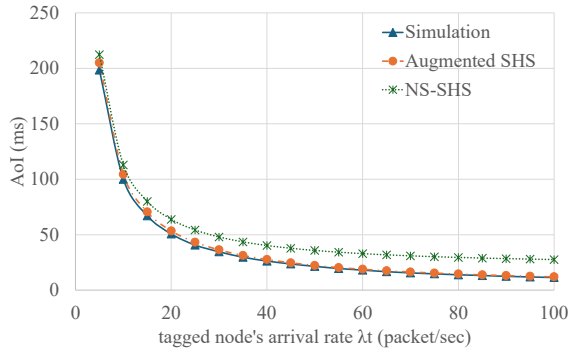

(a) $N = 5$.

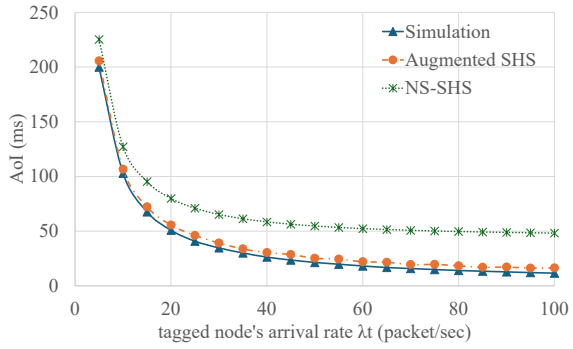

(b) $N = 10$.

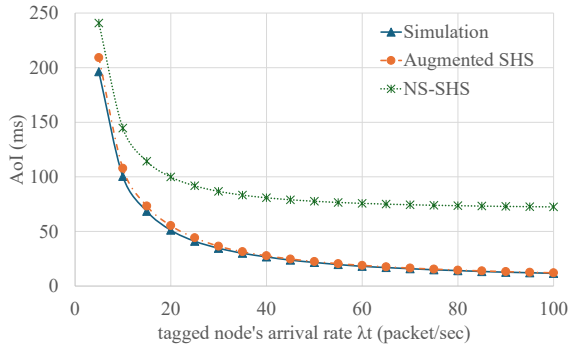

(c) $N = 15$.

Fig. 4. The tagged node's average AoI in unsaturated CSMA networks.

The above results clearly show the relationship between the tagged node's AoI and the traffic arrival rate. Increasing the arrival rate improves the AoI, but the improvement shows diminishing returns beyond a certain point.

D. Effectiveness of Sampling Cost vs. AoI Improvement

To better understand the trade-off between sampling cost and AoI improvement, we analyze how varying the sampling cost affects AoI reduction. Our analysis reveals diminishing returns in the age curves; beyond a certain point, increasing the arrival rate results in only marginal improvements in AoI. This emphasizes the need to find an optimal arrival rate that balances information freshness with the associated cost.

The age curve versus traffic arrival rate illustrates the varying impacts of arrival rates on AoI improvement. To quantify the effectiveness of sampling cost in relation to AoI

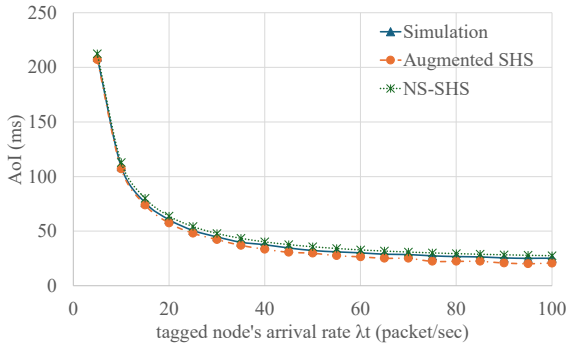

Fig. 5. The tagged node's average AoI in saturated CSMA with $N = 5$.

improvement, we define the "AoI reduction efficiency" (ARE) as

$$\delta = \frac{\Delta_{\text{AoI}}}{\Delta_\lambda}, \tag{11}$$

where Δ_{AoI} represents the reduction in AoI, and Δ_λ is the corresponding increase in the traffic arrival rate. This metric essentially measures the negative slope of the age curve, indicating the rate of change in AoI with respect to changes in the arrival rate. By using ARE, we can evaluate how efficiently an increase in sampling cost translates into AoI improvement, guiding the selection of an optimal arrival rate that minimizes AoI while considering cost constraints.

E. Joint Evaluation for AoI and Sampling Cost

Building on the previous analysis, it is evident that for a tagged node with a small queue, maintaining a low AoI typically requires a higher update arrival rate, which increases the sampling cost. A system designed to minimize only the AoI might lead to excessive resource consumption, resulting in higher operational costs. Conversely, focusing solely on reducing sampling costs may lead to outdated information, compromising the system's effectiveness. This trade-off necessitates a joint evaluation to find an optimal balance between minimizing AoI and controlling the sampling cost. In this context, "sampling cost" and "arrival rate" are used interchangeably because higher arrival rates result in more frequent updates, thus increasing the sampling cost.

To quantify the joint performance, we propose a composite metric denoted as P that combines both AoI and arrival rate:

$$P = \alpha\tilde{\Delta} + (1-\alpha)\tilde{\lambda}, \tag{12}$$

where

- α and $1-\alpha$ are weight factors that determine the importance of AoI and arrival rate, respectively.
- $\tilde{\Delta}$ is the normalized AoI.
- $\tilde{\lambda}$ is the normalized arrival rate.

To ensure that the AoI and arrival rate are on comparable scales, we normalize them using min-max normalization:

$$\tilde{\Delta} = \frac{\Delta - \Delta_{\min}}{\Delta_{\max} - \Delta_{\min}}, \quad \tilde{\lambda} = \frac{\lambda - \lambda_{\min}}{\lambda_{\max} - \lambda_{\min}}, \tag{13}$$

where $\Delta_{\max}$ is a quality of service (QoS) metric indicating the satisfactory threshold of a node regarding information freshness, and $\lambda_{\max}$ is the highest sampling rate a node can afford. $\Delta_{\min}$ and $\lambda_{\min}$ are typically set to 0. The weights α should be chosen based on the specific requirements or preferences of the system. For instance, if minimizing AoI is more critical, α should be tuned larger accordingly. The optimal policy is obtained by minimizing P.

Taking Fig. 4a as an example, the joint performance with various weights is demonstrated in Fig. 6 with $\Delta_{\max} = 198.48$ ms and $\lambda_{\max} = 100$ packet/sec. When α is smaller, minimizing P occurs at lower λ_t, guiding the tagged node to conserve sampling cost by prioritizing cost-saving over AoI performance. Conversely, with a higher α, minimizing P occurs at higher λ_t, encouraging the tagged node to increase the sampling rate for better AoI performance.

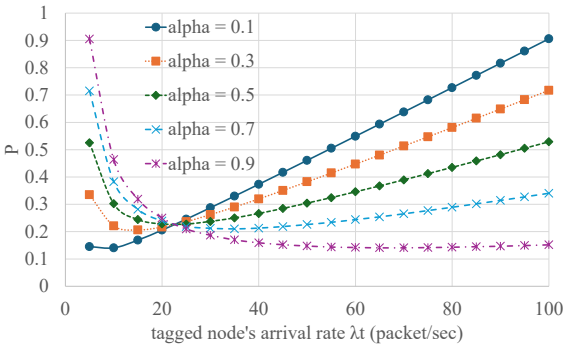

Fig. 6. Joint performance for AoI and sampling cost, an example for Fig. 4a.

This approach not only addresses the balance between AoI and sampling cost but also ensures that the framework remains adaptable and efficient across various network scenarios. This is particularly relevant for real-time applications where both information freshness and resource management are crucial. By incorporating dynamic adaptation through deep learning, the model provides a robust solution.

VI. Related Work

The critical role of AoI in CSMA networks has led to extensive research beyond conventional sampling strategies, packet management mechanisms, link scheduling, and different age metrics [21]–[37]. Kaul et al. [7] pioneer this field by examining vehicular networks, employing a small buffer and optimized broadcast periods to minimize system age, though their work is primarily simulation-based. Kadota et al. [38] focus on random access networks, optimizing the random access mechanism under stochastic packet generation and considering collision effects, with the assumption that sources retain only the freshest updates. Jiang et al. [39] utilize multi-agent reinforcement learning (MARL) to enhance data transmission efficiency, outperforming traditional MAC protocols in terms of both average and peak AoI. Meanwhile, Wang et al. [11], [40], [41] present analytical methods to reduce AoI for a tagged node in 802.11-based networks, focusing on service time approximation and arrival rate optimization, but these studies assume infinite buffer sizes. Additionally, Tripathi et al. [42] introduce Fresh-CSMA, a distributed protocol that emulates max-weight scheduling to minimize AoI in single-hop wireless networks. Zhou and Saad's work [43], [44] on ultra-dense IoT systems provides closed-form expressions for average and peak AoI, highlighting the advantages of preemptive schemes over non-preemptive ones. Fan et al. [45]–[47] combines second-order analysis and mean-field approximation for AoI minimization for distributed uplink transmissions in CSMA networks.

The SHS approach has gained traction for AoI analysis in CSMA networks due to its comprehensive modeling capabilities. Maatouk et al. [9] develop an SHS framework for analyzing AoI in collision-free heterogeneous CSMA networks, assuming instant sampling and immediate preemptive service while neglecting practical queuing effects. This model also approximates collision effects by bounding channel access time, without evaluating performance in collision-prone environments. Addressing these limitations, Wang et al. [10] introduce an SHS model that incorporates packet collisions and limited buffer scenarios for heterogeneous CSMA networks, providing insights into near-saturated conditions. However, this model's effectiveness in realistic unsaturated networks is restricted. Asvadi et al. [48] extend SHS analysis by deriving a general formula for average peak AoI (PAoI) applicable to various scenarios, including VANETs. Furthermore, Maatouk et al. [49] advance SHS modeling by allowing system transition dynamics to be polynomial functions of AoI, resulting in more sophisticated analysis and significant performance gains in age-aware CSMA environments compared to age-blind approaches. These advancements underscore the potential of SHS to enhance the precision and applicability of AoI analysis in CSMA networks.

VII. Conclusion

This work presents a novel DL-augmented SHS model for AoI analysis in both heterogeneous unsaturated and saturated CSMA networks. We address the limitations of the existing NS-SHS model, which often assumes near-saturated settings, by leveraging DL to dynamically refine the SHS model parameters, thereby improving estimation accuracy. Our approach is validated using 802.11-based simulations in the ns-3 simulator, demonstrating robustness and efficiency in practical CSMA scenarios. The results show significant improvements in AoI analysis accuracy compared to existing methods, particularly in unsaturated network conditions. Additionally, we introduce a joint evaluation metric to balance AoI and sampling cost, allowing for an optimal sampling strategy. This integration of SHS and DL provides a powerful and adaptable framework for AoI analysis, making it highly suitable for real-world applications in timeliness-critical systems.

VIII. Acknowledgment

This work was supported in part by the U.S. National Science Foundation (NSF) under Grant CNS-2008092.

REFERENCES

[1] S. Kaul, R. Yates, and M. Gruteser, "Real-time status: How often should one update?" in *Proc. of IEEE INFOCOM*, 2012, pp. 2731–2735.

[2] R. D. Yates and S. K. Kaul, "The age of information: Real-time status updating by multiple sources," *IEEE Transactions on Information Theory*, vol. 65, no. 3, pp. 1807–1827, 2019.

[3] R. D. Yates and S. Kaul, "Real-time status updating: Multiple sources," in *Proc. of IEEE ISIT*, 2012, pp. 2666–2670.

[4] Y. Sun, E. Uysal-Biyikoglu, R. D. Yates, C. E. Koksal, and N. B. Shroff, "Update or wait: How to keep your data fresh," *IEEE Transactions on Information Theory*, vol. 63, no. 11, pp. 7492–7508, 2017.

[5] R. D. Yates, "Lazy is timely: Status updates by an energy harvesting source," in *Proc. of IEEE ISIT*, 2015, pp. 3008–3012.

[6] A. Kosta, N. Pappas, A. Ephremides, and V. Angelakis, "Age and value of information: Non-linear age case," in *Proc. of IEEE ISIT*, 2017, pp. 326–330.

[7] S. Kaul, M. Gruteser, V. Rai, and J. Kenney, "Minimizing age of information in vehicular networks," in *Proc. of IEEE SECON*, 2011, pp. 350–358.

[8] L. Li, Y. Dong, C. Pan, and P. Fan, "Timeliness of wireless sensor networks with random multiple access," *Journal of Communications and Networks*, vol. 25, no. 3, pp. 405–418, 2023.

[9] A. Maatouk, M. Assaad, and A. Ephremides, "On the age of information in a CSMA environment," *IEEE/ACM Transactions on Networking*, vol. 28, no. 2, pp. 818–831, 2020.

[10] S. Wang, O. T. Ajayi, and Y. Cheng, "An analytical approach for minimizing the age of information in a practical CSMA network," in *Proc. of IEEE INFOCOM*, 2024, pp. 1721–1730.

[11] S. Wang and Y. Cheng, "A deep learning assisted approach for minimizing the age of information in a WiFi network," in *Proc. of IEEE MASS*, 2022, pp. 58–66.

[12] R. D. Yates, Y. Sun, D. R. Brown, S. K. Kaul, E. Modiano, and S. Ulukus, "Age of information: An introduction and survey," *IEEE Journal on Selected Areas in Communications*, vol. 39, no. 5, pp. 1183–1210, 2021.

[13] J. P. Hespanha, "Modelling and analysis of stochastic hybrid systems," *IEE Proceedings-Control Theory and Applications*, vol. 153, no. 5, pp. 520–535, 2006.

[14] G. Bianchi, "Performance analysis of the IEEE 802.11 distributed coordination function," *IEEE Journal on Selected Areas in Communications*, vol. 18, no. 3, pp. 535–547, 2000.

[15] H. Zhai, Y. Kwon, and Y. Fang, "Performance analysis of IEEE 802.11 MAC protocols in wireless LANs," *Wireless communications and mobile computing*, vol. 4, no. 8, pp. 917–931, 2004.

[16] S. Zhang, B. Yin, S. Wang, and Y. Cheng, "Robust deep learning for wireless network optimization," in *Proc. of IEEE ICC*, 2020, pp. 1–7.

[17] Y. Cheng, X. Ling, W. Song, L. X. Cai, W. Zhuang, and X. Shen, "A cross-layer approach for WLAN voice capacity planning," *IEEE Journal on Selected Areas in Communications*, vol. 25, no. 4, pp. 678–688, 2007.

[18] G. F. Riley and T. R. Henderson, "The ns-3 network simulator," *Modeling and tools for network simulation*, pp. 15–34, 2010.

[19] T. Akiba, S. Sano, T. Yanase, T. Ohta, and M. Koyama, "Optuna: A next-generation hyperparameter optimization framework," in *Proc. of the ACM SIGKDD*, 2019, pp. 2623–2631.

[20] A. Paszke, S. Gross, F. Massa, A. Lerer, J. Bradbury, G. Chanan, T. Killeen, Z. Lin, N. Gimelshein, L. Antiga *et al.*, "Pytorch: An imperative style, high-performance deep learning library," *Advances in neural information processing systems*, vol. 32, 2019.

[21] M. Costa, M. Codreanu, and A. Ephremides, "Age of information with packet management," in *Proc. of IEEE ISIT*, 2014, pp. 1583–1587.

[22] L. Huang and E. Modiano, "Optimizing age-of-information in a multi-class queueing system," in *Proc. of IEEE ISIT*, 2015, pp. 1681–1685.

[23] M. Costa, M. Codreanu, and A. Ephremides, "On the age of information in status update systems with packet management," *IEEE Transactions on Information Theory*, vol. 62, no. 4, pp. 1897–1910, 2016.

[24] J. Zhong, R. D. Yates, and E. Soljanin, "Two freshness metrics for local cache refresh," in *Proc. of IEEE ISIT*, 2018, pp. 1924–1928.

[25] A. Maatouk, S. Kriouile, M. Assaad, and A. Ephremides, "The age of incorrect information: A new performance metric for status updates," *IEEE/ACM Transactions on Networking*, vol. 28, no. 5, pp. 2215–2228, 2020.

[26] Y. Sun and B. Cyr, "Information aging through queues: A mutual information perspective," in *Proc. of IEEE SPAWC*, 2018, pp. 1–5.

[27] B. Yin, S. Zhang, Y. Cheng, L. X. Cai, Z. Jiang, S. Zhou, and Z. Niu, "Only those requested count: Proactive scheduling policies for minimizing effective age-of-information," in *Proc. of IEEE INFOCOM*, 2019, pp. 109–117.

[28] B. Yin, S. Zhang, and Y. Cheng, "Application-oriented scheduling for optimizing the age of correlated information: A deep-reinforcement-learning-based approach," *IEEE Internet of Things Journal*, vol. 7, no. 9, pp. 8748–8759, 2020.

[29] Y. Sun and B. Cyr, "Sampling for data freshness optimization: Non-linear age functions," *Journal of Communications and Networks*, vol. 21, no. 3, pp. 204–219, 2019.

[30] S. Zhou and X. Lin, "An easier-to-verify sufficient condition for whittle indexability and application to AoI minimization," in *Proc. of IEEE INFOCOM*, 2024, pp. 1741–1750.

[31] ——, "On the active-time condition for partial indexability and application to heterogeneous-channel AoI minimization," in *Proc. of ACM MobiHoc*, 2024, p. 311–320.

[32] X. Chen, K. Gatsis, H. Hassani, and S. S. Bidokhti, "Age of information in random access channels," *IEEE Transactions on Information Theory*, pp. 1–1, 2022.

[33] Q. He, G. Dán, and V. Fodor, "Joint assignment and scheduling for minimizing age of correlated information," *IEEE/ACM Transactions on Networking*, vol. 27, no. 5, pp. 1887–1900, 2019.

[34] D. Guo, K. Nakhleh, I.-H. Hou, S. Kompella, and C. Kam, "A theory of second-order wireless network optimization and its application on AoI," in *Proc. of IEEE INFOCOM*, 2022, pp. 999–1008.

[35] ——, "AoI, timely-throughput, and beyond: A theory of second-order wireless network optimization," *IEEE/ACM Transactions on Networking*, vol. 32, no. 6, pp. 4707–4721, 2024.

[36] P. Mollahosseini, S. Asvadi, and F. Ashtiani, "Effect of variable backoff algorithms on age of information in slotted ALOHA networks," *IEEE Transactions on Mobile Computing*, vol. 23, no. 9, pp. 8620–8633, 2024.

[37] J. Luo and N. Pappas, "Minimizing the age of missed and false alarms in remote estimation of markov sources," in *Proc. of ACM MobiHoc*, 2024, pp. 381–386.

[38] I. Kadota and E. Modiano, "Age of information in random access networks with stochastic arrivals," in *Proc. of IEEE INFOCOM*, 2021, pp. 1–10.

[39] Z. Jiang, Y. Liu, J. Hribar, L. A. DaSilva, S. Zhou, and Z. Niu, "SMART: Situationally-aware multi-agent reinforcement learning-based transmissions," *IEEE Transactions on Cognitive Communications and Networking*, vol. 7, no. 4, pp. 1430–1443, 2021.

[40] S. Wang, Y. Cheng, L. X. Cai, and X. Cao, "Minimizing the age of information for monitoring over a WiFi network," in *Proc. of IEEE GLOBECOM*, 2022, pp. 383–388.

[41] S. Wang, "Machine learning-assisted age of information optimization in practical CSMA-based wireless networks," Ph.D. dissertation, Illinois Institute of Technology, 2024.

[42] V. Tripathi, N. Jones, and E. Modiano, "Fresh-CSMA: A distributed protocol for minimizing age of information," in *Proc. of IEEE INFOCOM*, 2023, pp. 1–10.

[43] B. Zhou and W. Saad, "Performance analysis of age of information in ultra-dense internet of things (IoT) systems with noisy channels," *IEEE Transactions on Wireless Communications*, vol. 21, no. 5, pp. 3493–3507, 2022.

[44] ——, "Age of information in ultra-dense IoT systems: Performance and mean-field game analysis," *IEEE Transactions on Mobile Computing*, vol. 23, no. 5, pp. 4533–4547, 2024.

[45] S. Fan, Y. Zhong, I.-H. Hou, and C. Kam, "Minimizing moments of AoI for both active and passive users through second-order analysis," in *Proc. of IEEE ISIT*, 2023, pp. 951–956.

[46] S. Fan, Y. Zhong, I.-H. Hou, and C. K. Kam, "Optimizing age of information in random access networks: A second-order approach for active/passive users," *IEEE Transactions on Communications*, pp. 1–1, 2024.

[47] S. Fan and I. Hou, "Second-order analysis of CSMA protocols for age-of-information minimization," in *Proc. of IEEE ACSSC*, 2024, to appear.

[48] S. Asvadi and F. Ashtiani, "Evaluating peak age-of-information via stochastic hybrid systems," *IEEE Transactions on Vehicular Technology*, vol. 72, no. 12, pp. 16 923–16 928, 2023.

[49] A. Maatouk, M. Assaad, and A. Ephremides, "Age-aware stochastic hybrid systems: Stability, solutions, and applications," *IEEE Journal on Selected Areas in Information Theory*, vol. 4, pp. 762–783, 2023.